Supporting Information

Chiang et al. 10.1073/pnas.1002176107

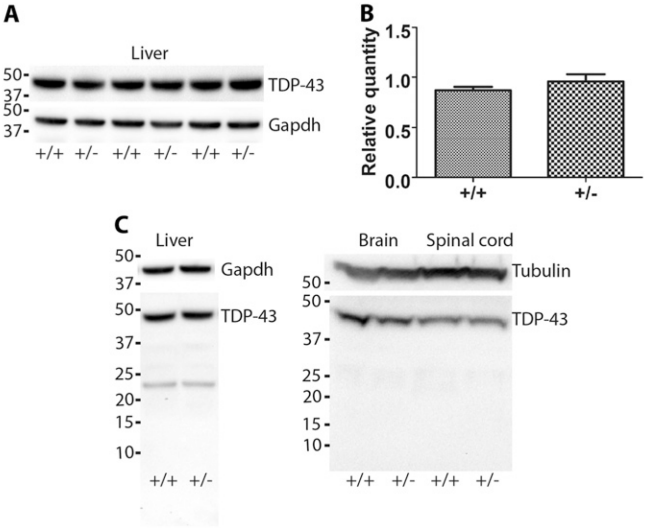

Fig. S1. Levels of TDP-43 in *Tardbp*$^{+/-}$ mice. (*A*) Tissue lysates of livers harvested from 6-wk-old control and *Tardbp*$^{+/-}$ mice were subjected to protein blot analysis using antisera against TDP-43. The blot was reprobed using an antibody to GAPDH. (*B*) Note comparable levels of TDP-43 were observed in the liver tissues between *Tardbp*$^{+/-}$ mice and control mice ($n = 3$ pairs of independent animals, mean ± SEM). (*C*) Lysates of liver, brain, and spinal cord from control and *Tardbp*$^{+/-}$ mice subjected to protein blot analysis using an anti–N-terminal TDP-43 antibody. Note that we failed to detect any putative N-terminal fragments of TDP-43 of the predicted molecular weight as a result of deletion of exon 3 in *Tardbp*$^{+/-}$ mice. An approximate 20 to 25 kDa band observed in liver extract of *Tardbp*$^{+/-}$ mice is likely nonspecific considering the similar band intensities also seen in that of control. Anti-GAPDH and anti–α-tubulin antisera served as the loading controls for liver and brain/spinal cord, respectively.

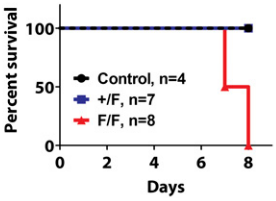

Fig. S2. Rapid lethality in *R26-ErCre;Tardbp*$^{F/F}$ mice. Kaplan-Meier survival plot of control, *R26-ErCre;Tardbp*$^{+/F}$, and *R26-ErCre;Tardbp*$^{F/F}$ mice following treatment with tamoxifen diet.

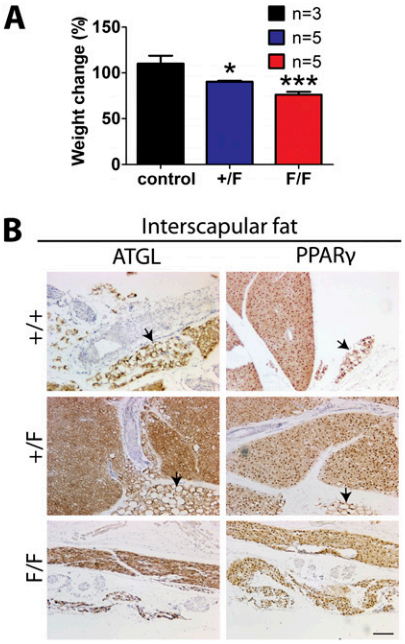

Fig. S3. Body weights and immunocytochemical analysis of adipocytes of the *CAG-ErCre;Tardbp*$^{+/F}$ and *CAG-ErCre;Tardbp*$^{F/F}$ mice. (*A*) Relative body weight to d 0 (pretreatment) of control, *CAG-ErCre;Tardbp*$^{+/F}$, and *CAG-ErCre;Tardbp*$^{F/F}$ mice induced with tamoxifen diet for 18 d. (*B*) Immunohistochemical staining using the adipocyte-specific markers ATGL (*Left*) and PPAR-γ (*Right*) to visualize adipocytes (arrows) found in the interscapular fat. Arrows indicate well formed fat vacuoles in the control and *CAG-ErCre;Tardbp*$^{+/F}$ mice. Note the positive immunoreactivities of adipocyte markers in the *CAG-ErCre;Tardbp*$^{F/F}$ mice. (Scale bar: 100 μm.)

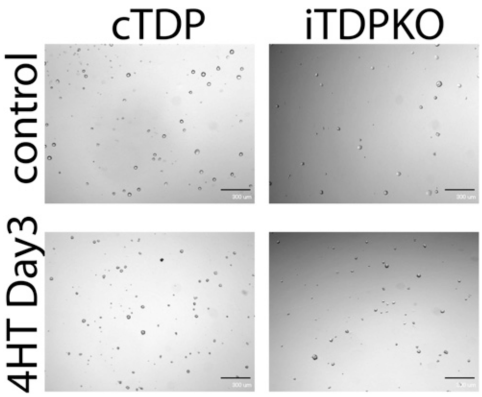

Fig. S4. Morphology of cTDP and iTDPKO ES cells. Photomicrographs of cTDP and iTDPKO ES cells before (*Upper*) and 3 d after (*Lower*) 4-HT treatment (100 ng/mL). Note the normal morphology for both groups of 4-HT–treated cells. (Scale bar: 300 μm.)

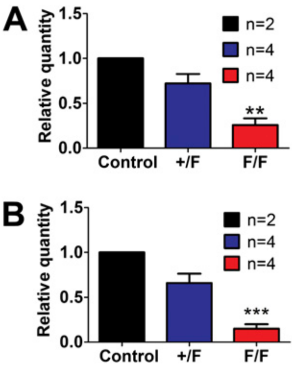

Fig. S5. Quantification of Tbc1d1 level in the skeletal muscle of *Tardbp* conditional KO mice. Level of TDP-43 (*A*) and Tbc1d1 (*B*) in the hindlimb skeletal muscles of induced *CAG-ErCre;Tardbp*$^{+/F}$ and *CAG-ErCre;Tardbp*$^{F/F}$ mice compared with control mice. Note the dramatic reduction of TDP-43 and Tbc1d1 in *CAG-ErCre;Tardbp*$^{F/F}$ mice (n = 4), whereas trends toward reduction of TDP-43 and Tbc1d1 were observed in the *CAG-ErCre;Tardbp*$^{+/F}$ mice (n = 4) compared with control mice (n = 2), although this decrease was not significant in *CAG-ErCre;Tardbp*$^{+/F}$ mice by ANOVA with Dunnett post analysis.

Table S1. **Top 30 low *P* value hits of differentially expressed genes identified between control and Tardbp-KO ES cells**

Gene symbol	iTDPKO-1 (RPKM)	iTDPKO-2 (RPKM)	iTDPKO-3 (RPKM)	cTDP-1 (RPKM)	cTDP-2 (RPKM)	Fold change	*P* value
9030409G11Rik	0.522758	0.805848	0.536447	11.2826	12.7248	−17.9599	4.05e−195
Tardbp	0.268818	0.363782	0.25103	4.21705	3.90988	−13.6264	5.82e−84
Fam73a	0.81858	0.874048	0.886107	8.52423	5.5301	−9.37043	7.43e−128
Tbc1d1	2.20639	2.07653	2.33996	16.0067	15.8936	−7.35415	7.02e−228
Rfc2	9.23564	11.0367	11.79	71.8	73.0135	−6.92943	1.30e−277
Med27	4.13347	3.01464	4.92048	24.8943	27.4378	−6.68084	6.05e−79
Pknox2	1.54048	1.37413	2.7521	10.8823	5.69187	−5.97637	2.11e−81
Usp15	3.65154	3.2335	3.59843	20.2915	19.0505	−5.78478	1.17e−146
Gnas	2.66274	2.58464	5.85189	17.5535	17.437	−5.58237	7.22e−69
Ascc1	8.37677	8.40692	7.02357	43.7665	43.3	−5.34497	3.81e−136
Tecpr1	1.52394	1.53052	1.72217	7.15085	8.37977	−4.72988	9.36e−61
Ptcd2	6.76655	6.78224	8.22956	29.4082	34.7043	−4.33227	3.80e−92
Glb1	30.5991	23.6241	42.1448	124.719	134.641	−4.28104	0
Pnpla6	2.22874	3.95951	4.15322	13.7981	11.0422	−4.086	3.67e−101
Ppp2r5c	5.7492	3.33226	9.12782	20.6639	20.276	−3.89642	1.13e−140
A230046K03Rik	1.77563	2.01244	1.74188	6.97357	6.94853	−3.72948	3.13e−64
Abr	3.75746	1.9821	4.63272	10.2884	16.8955	−3.63079	1.01e−88
Radil	3.59818	3.81858	4.05638	14.3332	9.35929	−3.57204	9.71e−74
Raly	11.5752	4.03739	4.90926	29.7497	8.81486	−3.52495	1.53e−65
Hdac6	5.36254	4.09085	10.0862	20.1262	17.0858	−3.50291	1.68e−117
Cnot2	11.7117	6.94643	15.6948	33.8795	40.3145	−3.37867	4.02e−133
Acin1	10.4665	5.6133	4.338	23.9081	30.5742	−3.36105	1.15e−82
Heatr5b	3.15116	2.508	3.17054	9.48398	9.85523	−3.30815	1.26e−83
Wdhd1	5.99969	5.60904	6.17496	18.2836	19.6844	−3.15999	1.97e−97
Katna1	9.96776	9.57181	9.91048	31.135	27.7413	−3.11689	7.86e−68
Abr	4.83957	5.43079	2.99213	15.5382	10.2372	−3.04585	5.56e−93
Ss18	36.4408	41.993	41.8575	11.561	16.1623	3.19853	5.62e−134
Uhrf1	29.4234	23.267	22.3903	5.81243	12.7337	3.64959	1.33e−114
Rpa3	75.2287	133.297	52.7848	22.9925	28.1976	4.00289	8.32e−88
Ddef2	5.95374	6.01087	5.51807	0.63628	1.82683	6.95352	6.55e−71

Genes with more than threefold increase or decrease are shown here. Individual RPKM for each sample are indicated. RKPM, reads per kilobase exon model per million mapped reads.

Table S2. **Summary of RNA-sequencing output**

	Raw reads	Mapped reads	Align (PF), %	Alignment score (PF)	Error rate (PF), %
iTDPKO-1	16,753,111	11,318,402	67.56 ± 0.35	77.12 ± 1.43	0.80 ± 0.25
iTDPKO-2	16,376,081	11,068,593	67.59 ± 3.11	76.45 ± 4.04	0.84 ± 0.18
iTDPKO-3	6,894,876	4,298,955	62.35 ± 9.37	64.48 ± 12.74	1.95 ± 0.98
cTDP-1	15,211,355	10,214,425	67.15 ± 0.38	75.39 ± 1.20	0.86 ± 0.18
cTDP-2	3,554,955	2,240,688	63.03 ± 7.51	65.59 ± 10.29	2.07 ± 0.88

Table S3. Pathway analysis of overlapping genes by RNA-seq. Only differential expressed genes with $P < e^{-20}$ were included for pathway analysis

KEGG pathway	Gene number	Entrez Gene IDs	*P* value*
Ribosome	15	19941 19946 19988 20044 20055 20088 20103 22121 26961 270106 27207 5604065019 67115 67891	2.45e−7
Focal adhesion	11	110157 11461 11465 14268 16776 16777 170736 192176 22339 226519 286940	1.28e−2
Cell cycle	10	15182 17120 17215 17216 18538 22059 22627 22628 59008 66156	5.71e−3
MAPK signaling pathway	9	110157 11911 14175 15481 19056 192176 19252 22059 286940	3.78e−1
Oxidative phosphorylation	8	11947 11984 12867 17992 57423 66091 66144 66416	4.02e−2
Calcium signaling pathway	7	11739 12314 14683 16440 19056 22334 53313	6.91e−2
Insulin signaling pathway	7	110157 12314 14252 18746 22084 26987 56421	1.44e−1
Pyrimidine metabolism	6	110074 20020 50493 59001 69719 70428	5.07e−2
Antigen processing and presentation	6	12317 12330 13039 15481 15516 15519	1.76e−3
Cell Communication	6	11461 11465 14268 16776 16777 226519	7.43e−3
Regulation of actin cytoskeleton	6	110157 11461 11465 14175 14268 18643	4.54e−1
Wnt signaling pathway	5	12301 19056 20377 21372 22059	4.47e−1
Tight junction	5	11461 11465 13821 56449 67374	2.71e−1
Long-term potentiation	5	110157 11911 12314 16440 19056	4.35e−2
Glycolysis/Gluconeogenesis	5	13806 15275 15277 18746 56421	3.46e−2
Purine metabolism	5	14450 18746 20020 59001 70428	3.93e−1
GnRH signaling pathway	5	110157 11911 12314 14683 16440	1.66e−1
Huntington’s disease	4	12314 12411 12757 22059	9.37e−3
Leukocyte transendothelial migration	4	11461 11465 18613 67374	2.97e−1
Gap junction	4	110157 14683 16440 22152	2.11e−1
Cell adhesion molecules (CAMs)	4	12550 17967 18613 67374	1.79e−1
ECM-receptor interaction	4	14268 16776 16777 226519	9.58e−2
Axon guidance	4	13845 13846 140570 19056	5.23e−1
Proteasome	4	17463 19185 26440 26441	2.46e−2
Glutathione metabolism	4	14776 14860 14862 15926	2.75e−2
Selenoamino acid metabolism	4	12411 15469 20768 232087	1.10e−2
Pancreatic cancer	4	110157 19730 22059 22339	2.36e−1
Galactose metabolism	4	12091 15275 15277 56421	1.93e−2

Red type indicates $P < 0.05$. KEGG, Kyoto Encyclopedia of Genes and Genomes.

*Determined by hypergeometric test.